Random patterns of non-overlapping convex grains

August 19, 2001

Marianne Månsson and Mats Rudemo

Department of Mathematical Statistics, Chalmers University of Technology, SE – 412 96 Gothenburg, Sweden

E-mail: marianne@math.chalmers.se and rudemo@math.chalmers.se

Abstract

Generalizing Matérn's (1960) two hard-core processes, marked point processes are considered as models for systems of varying-sized, non-overlapping convex grains. A Poisson point process is generated and grains are placed at the points. The grains are supposed to have varying sizes but the same shape as a fixed convex grain — with spheres as an important special case. The pattern is thinned so that no grains overlap. We consider the thinning probability of a "typical point" under various thinning procedures, the volume fraction of the resulting system of grains, the relation between the intensity of the point processes before and after thinning, and the corresponding size distributions. The study is inspired by problems in material fatigue, where cracks are supposed to be initiated by large defects.

Keywords: Germ-grain process, non-overlapping grains, radius distribution, Poisson process, volume fraction, material fatigue, Matérn's hard-core processes.

AMS 2000 Subject Classification: Primary 60D05
Secondary 60G55, 62M30

1 Introduction

In his seminal work Matérn (1960) introduced two point processes with a fixed minimal distance between points. These processes are obtained in two steps.

First a stationary Poisson point process is generated. Then the point pattern is thinned such that no points are closer than the fixed minimal distance D. To obtain Matérn's first model every point with its nearest neighbour closer than D is excluded. In the second model weights are independently assigned to the points according to a uniform distribution over (0,1). A point is then kept if there is no other point with a higher weight within the distance D. By regarding the remaining points of the point pattern as centres of spheres with diameter equal to the minimal inter-point distance, we can interpret Matérn's two constructions as models for random patterns of non-overlapping spheres with fixed radii.

Both these processes are in the present paper generalized from fixed-sized spheres to convex grains of varying sizes. First we consider spheres, but the treatment is structured so that items that need to be modified later on for convex grains are easily identified. In this way we hope to facilitate the exposition, which might have been rather technical if we had gone directly to the patterns with convex grains. Furthermore, the first model is generalized in the following manner: instead of removing both points if they are closer to each other than the distance D, weights are assigned to the two points and the one with the lower weight is removed (both if their weights are equal). This is done for all "close pairs", and hence one point might get different weights in the "competition" with different points. This is called pairwise assignment of weights below, while the assignment in the second model is called global. Finally, in both models we allow the weights to have a more general distribution, and possibly depend on the radii of the corresponding spheres.

In Section 2 we define the processes of varying-sized spheres with either pairwise or global assignment of weights, and we obtain the thinning probabilities for a sphere of a given size for the two cases. These results are used in Section 3 to compute the intensity of the point process of sphere centres and the sphere radius distribution after thinning. It is shown that under certain conditions the right tail of the "proposal" radius distribution is asymptotically retained. Special cases for which explicit results are obtained include the exponential distribution in dimension one, the truncated normal distribution in dimension two, and mixture models with two sphere sizes. An iterative inversion algorithm for the radius distribution is suggested and found to perform satisfactorily in an example.

The models are generalized to processes of convex grains in Section 4.

We consider both grains with a fixed orientation and grains with a purely random orientation. For fixed orientations and also fixed sizes we find in Section 4.3 inequalities for the maximal volume fraction of the union of all grains, in the case of a uniform weight distribution. The upper bound is attained for centrally symmetric grains (e.g. rectangles and ellipses in $\mathbb{R}^2$), while the lower bound is attained for simplexes (i.e. triangles in $\mathbb{R}^2$).

In the final Section 5, we briefly discuss some possible future directions of research, including study of second order characteristics and asymptotic properties of large grains, and the modelling of inclusion data.

The present study is inspired by problems of fatigue in steel and cast iron, cf. Murakami and Beretta (1999), where it is discussed how fatigue strength is related to the size of the maximum defects in specimens. Defects of spherical shape are natural for some applications such as cast iron, but for other applications it is more relevant to consider non-spherical defects. In particular, for rolled steel it is quite natural to consider defects with a fixed orientation, cf. Zoughi et al. (1997).

Figure 1 shows images from Beretta (2000) of two 2D-cuts in cast iron with defects which are close to being disc-shaped. These images indicate that the corresponding distribution of defects in 3D could to a good approximation be described as a pattern of varying-sized spheres.

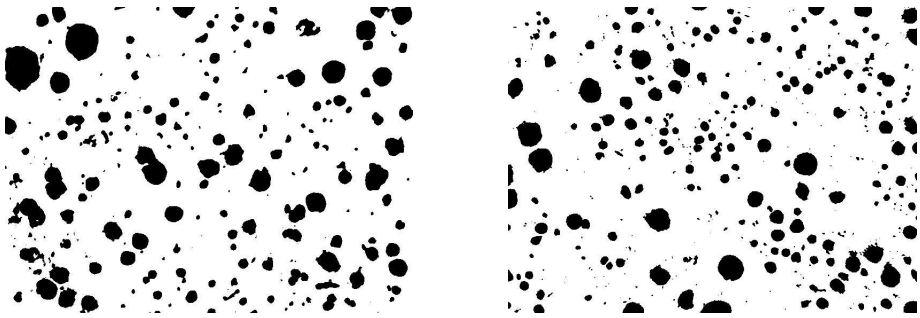

Figure 1: Two cuts in cast iron showing approximately disc-shaped defects

There is a large literature on processes of non-overlapping grains in physics and chemistry. One such application area is random sequential adsorption, RSA, cf. the recent review paper by Talbot et al. (2000). In the statistical literature this model is often called simple sequential inhibition, SSI.

For variable sized spheres, Meakin and Jullien (1992a, 1992b) study random sequential adsorption in two and three dimensions. Another extensively studied area consists of Gibbsian systems of spheres, see for instance Reiss, Frisch and Lebowics (1959) and Torquato (1995). Possible size distributions in Gibbs processes of discs are studied in Mase (1985).

Random patterns of non-overlapping spheres have been studied for several decades in spatial statistics and stochastic geometry, cf. Stoyan, Kendall and Mecke (1995) and Stoyan (1998). The Stienen model originating from material science applications (Stienen, 1982) allows fairly detailed theoretical analysis (Stoyan, 1990). This model gives a germ-grain process with germ positions forming a Poisson process. Another such process is obtained from the dynamic lily-pond model, see Häggström and Meester (1996) and Daley, Stoyan and Stoyan (1999).

A model closely related both to random sequential adsorption and to Matérn's second model is Matheron's dead leaves model, cf. Jeulin (1998) and Stoyan and Schlater (2000). Here germ points are placed randomly according to a Poisson process in time and space. In each germ point a grain is placed, and if several grains cover a given position in space, only the most recently placed grain is visible at that position.

2 Definition of the processes of varying-sized spheres

A process of d-dimensional spheres in Euclidean d-space $\mathbb{R}^d$ is regarded as a marked point process with the radius of a sphere centred at a point of the point process as the mark of that point. Let us regard marked point processes constructed in two steps as follows.

In the first step we generate a Poisson point process with constant intensity λ in $\mathbb{R}^d$, and to each point in this point process we generate identically distributed radii with a *proposal* distribution function F_{pr}. The radii are independent mutually and of the point process. This marked Poisson process we denote by Ψ. A point of a marked point process in $\mathbb{R}^d$ is denoted $[x; r]$, where $x \in \mathbb{R}^d$ is the position of the point and r is the mark, in our case the radius $r \in \mathbb{R}^+$, corresponding to the point.

In the second step we thin the marked point process by letting all pairs of points whose associated spheres intersect 'compete'. A point is kept if it has higher weight in all pairwise comparisons, where the, possibly random, weights are assigned to the points according to two different approaches:
1) *Pairwise assignment of weights*: For each comparison, weights are assigned to the involved pair of points, and assignments are independent both within and between pairs.
2) *Global assignment of weights*: Weights are assigned once and for all to all points, and assignments to different points are independent. These weights are then used in all comparisons.
In both cases the weight of a point may depend on the associated radius. When the weights are constant or deterministic functions of the radii, the two approaches coincide. Two such examples are given in Examples 2.1 and 2.2.

Some further notation is needed. Let $B_d(z,r) = \{x \in \mathbb{R}^d : |z-x| \leq r\}$ denote the d-dimensional ball centred at z with radius r, and let κ_d denote the volume of the unit ball in $\mathbb{R}^d$. Then $r^d\kappa_d$ is the volume of $B_d(z,r)$. Let o denote the origin. For an arbitrary distribution function F of a random variable X we further define $\bar{F}(x) = 1 - F(x-0) = \Pr(X \geq x)$.

2.1 Thinning probabilities

Consider a randomly chosen point, sometimes called a typical point (Stoyan et al., 1995, p. 108) of the original marked point process Ψ. Let r be the associated radius of this point and let $g_P(r)$ denote the retaining probability of the point, that is the probability that such a point is not deleted in the second step, when the pairwise approach is used. Let $g_G(r)$ denote the corresponding probability in the global case. Thus $1 - g_P(r)$ and $1 - g_G(r)$ are the thinning probabilities.

2.1.1 Pairwise assignment of weights

Given a pair of points with associated radii $[x_1; r_1], [x_2; r_2] \in \Psi$, we give the points independent weights, $W_1(r_1)$ and $W_2(r_2)$, with distribution functions $F_{W|r_1}$ and $F_{W|r_2}$, respectively, which may depend on the radii. If their associated spheres intersect, the point with the lower weight is removed, and if their weights are equal both points are removed.

Theorem 2.1 *Using the notation introduced above, the retaining probability in case of pairwise thinning is*

$$g_P(r) \;=\; \exp\{-\lambda\kappa_d \int_0^\infty Pr(W_1(r) \le W_2(y))(r+y)^d F_{pr}(dy)\},$$

where $W_1(r)$ and $W_2(y)$ are independent and have distribution functions $F_{W|r}$ and $F_{W|y}$, respectively.

Proof. Let $g_P(r,x)$ denote the probability that a randomly chosen point in Ψ, say $[z;r]$, with associated radius r, is retained in the second step when Ψ is restricted to the ball $B_d(z,x)$. Then $g_P(r,x) \to g_P(r)$ as $x \to \infty$ for any $r > 0$. Without loss of generality, it is enough to consider the case where z is the origin.

Since Ψ is a marked Poisson process with intensity λ, the number of points of Ψ which lie in $B_d(o,x)$, given that there is a point at the origin, is Poisson distributed with parameter $\lambda\kappa_d x^d$. Let X have a uniform distribution in $B_d(o,x)$, let R have distribution function F_{pr}, and note that $\Pr(B_d(o,r) \cap B_d(X,y) \neq \emptyset) = 1$ if $r + y > x$. Then we find

$$\begin{aligned}
&\Pr([o;r] \text{ removed by } [X;R]) \\
&= \int_0^\infty \Pr([o;r] \text{ removed by } [X;y]) F_{pr}(dy) \\
&= \int_0^\infty \Pr([o;r] \text{ removed by } [X;y]) \mid B_d(o,r) \cap B_d(X,y) \neq \emptyset) \\
&\quad \Pr(B_d(o,r) \cap B_d(X,y) \neq \emptyset) F_{pr}(dy) \qquad (2.1) \\
&= \int_0^\infty \Pr(W_1(r) \le W_2(y)) \Pr(X \in B_d(o, r+y)) F_{pr}(dy) \\
&= \int_0^\infty \Pr(W_1(r) \le W_2(y)) \min\left(\left(\frac{r+y}{x}\right)^d, 1\right) F_{pr}(dy).
\end{aligned}$$

Since the points in $B_d(o,x)$ remove $[o;r]$ independently of each other, the number of points with associated spheres which remove $[o;r]$ is Poisson distributed with parameter

$$\lambda\kappa_d x^d \int_0^\infty \Pr(W_1(r) \le W_2(y)) \min\left(\left(\frac{r+y}{x}\right)^d, 1\right) F_{pr}(dy) \;=$$
$$\lambda\kappa_d \int_0^\infty \Pr(W_1(r) \le W_2(y)) \min\big((r+y)^d, x^d\big) F_{pr}(dy).$$

The point $[o; r]$ is retained if the number of points which removes it is zero; thus

$$g_P(r, x) \;=\; \exp\{-\lambda\kappa_d \int_0^\infty \Pr(W_1(r) \le W_2(y))\, \min\big((r+y)^d, x^d\big)\, F_{pr}(dy)\}.$$

Let $x \to \infty$ in both sides of this equation to complete the proof. ■

The following corollary follows immediately, since for any continuous weight distribution $F_{W|r}$, which does not depend on r, we have $\Pr(W_1(r) \le W_2(y)) = 1/2$.

Corollary 2.2 *For any continuous weight distribution $F_{W|r}$, which does not depend on r,*

$$g_P(r) \;=\; \exp\{-\lambda\kappa_d \frac{1}{2} \int_0^\infty (r+y)^d F_{pr}(dy)\}.$$

In the following two examples the weights are constant or deterministic functions of the radii. As mentioned previously, the pairwise and global thinning procedures result in the same process in such cases.

Example 2.1. *Intersecting spheres removed.* A point and its associated d-dimensional sphere are kept if and only if the sphere meets none of the other spheres of the original marked point process. Thus if two or more spheres have nonempty intersections in the first step those spheres are deleted in the second step. This can be achieved by giving the same weight to all points; then no point has a lower weight than another, so that $\Pr(W_1(r) \le W_2(y)) = 1$ and we get

$$g_P(r) \;=\; \exp\{-\lambda\kappa_d \int_0^\infty (r+y)^d F_{pr}(dy)\}.$$

If the radii are all equal, the resulting thinned point process is one of the processes suggested by Matérn (1960). □

Example 2.2. *Large spheres kept.* A point and its associated d-dimensional sphere are kept if and only if the sphere meets no larger or equal sized sphere

of the original marked point process. This is achieved by letting the weights equal the radius. Then $\Pr(W_1(r) \leq W_2(y)) = 1\{r \leq y\}$, and

$$g_P(r) \;=\; \exp\{-\lambda\kappa_d \int_r^\infty (r+y)^d F_{pr}(dy)\}.$$

We note that if the radius R has finite moment of dth order, $\mathbf{E}(R^d) < \infty$, then

$$\lim_{r\to\infty} g_P(r) = 1,$$

a result which will turn out to be quite useful in the sequel, see Corollary 3.3. □

2.1.2 Global weights

In this section we assign weights to the points once, and these weights are then used in all pairwise comparisons. As before, we let the weight have distribution function $F_{W|r}$, for a point with associated radius r.

Theorem 2.3 *Using the notation introduced above, the retaining probability in case of global thinning is*

$$\begin{aligned} g_G(r) &= \int_0^\infty \exp\{-\lambda\kappa_d \int_0^\infty \bar{F}_{W|y}(w)(r+y)^d F_{pr}(dy)\} F_{W|r}(dw) \\ &= \mathbf{E}[\exp\{-\lambda\kappa_d \int_0^\infty \bar{F}_{W|y}(W_1(r))(r+y)^d F_{pr}(dy)\}], \end{aligned}$$

where $W_1(r)$ has distribution function $F_{W|r}$.

Proof. Let $g_G(r,x)$ denote the probability that a randomly chosen point in Ψ, say $[z;r]$, with associated radius r is retained in the second step when Ψ is restricted to the ball $B_d(z,x)$. As in the proof of Theorem 2.1 we assume that $z = o$ and we let X have a uniform distribution on $B_d(o,x)$. Let R and $W(R)$ have distribution functions F_{pr} and $F_{W|R}$, respectively.

In this proof we let the marks of the point process Ψ consist of two parts: the associated radius and the weight. A point and its mark is denoted by

$[z; r, w]$. Similar arguments as in the proof of Theorem 2.1 give

$$\begin{aligned}
&\Pr([o; r, w] \text{ removed by } [X; R, W(R)] \\
&= \int_0^\infty \Pr([o; r, w] \text{ removed by } [X; y, W] \mid B_d(o, r) \cap B_d(X, y) \neq \emptyset) \\
&\quad \Pr(B_d(o, r) \cap B_d(X, y) \neq \emptyset) F_{pr}(dy) \qquad (2.2) \\
&= \int_0^\infty \bar{F}_{W|y}(w) \min\left(\left(\frac{r+y}{x} \right)^d, 1 \right) F_{pr}(dy),
\end{aligned}$$

and we get

$$\Pr([o; r, w] \text{ not removed}) = \exp\{-\lambda\kappa_d \int_0^\infty \bar{F}_{W|y}(w) \min\big((r+y)^d, x^d\big) F_{pr}(dy)\}.$$

To get $g_G(r, x)$ we integrate over the weights:

$$g_G(r, x) = \int_0^\infty \exp\{-\lambda\kappa_d \int_0^\infty \bar{F}_{W|y}(w) \min\big((r+y)^d, x^d\big) F_{pr}(dy)\} F_{W|r}(dw),$$

and the result follows by letting $x \to \infty$ in both sides of this equation. ■

If the weights are continuous random variables which are independent of each other and of the radii, we get a point process which is similar to one suggested by Stoyan and Stoyan (1985), called Model II in that article. As in their model, the choice of distribution function for the weights does not matter as long as it is continuous.

Corollary 2.4 *If the weight distribution $F_{W|r}$ is continuous and does not depend on r, then*

$$g_G(r) = \frac{1 - \exp\{-\lambda\kappa_d \int_0^\infty (r+y)^d F_{pr}(dy)\}}{\lambda\kappa_d \int_0^\infty (r+y)^d F_{pr}(dy)}.$$

Example 2.3. *Fixed radius.* For a fixed radius r and a weight distribution that is continuous, we get

$$g_G(r) = \frac{1 - \exp\{-\lambda\kappa_d (2r)^d\}}{\lambda\kappa_d (2r)^d}.$$

Note that this point process coincides with the second type of Matern's point processes with a minimal inter-point distance. □

2.1.3 Comparisons

Note that in the global approach $g_G(r)$ can be written as

$$g_G(r) = \mathbf{E}[\exp\{-\lambda\kappa_d \int_0^\infty \bar{F}_{W|y}(W_1(r))(r+y)^d F_{pr}(dy)\}], \qquad (2.3)$$

where the expectation $\mathbf{E}$ operates on the random variable $W_1(r)$ with distribution $F_{W|r}$. We can correspondingly write $\Pr(W_1(r) \leq W_2(y)) = \mathbf{E}[\bar{F}_{W|y}(W_1(r))]$ in the pairwise approach, and thus

$$g_P(r) = \exp\{-\lambda\kappa_d \int_0^\infty \mathbf{E}[\bar{F}_{W|y}(W_1(r))](r+y)^d F_{pr}(dy)\}. \qquad (2.4)$$

By Jensen's inequality the following result follows from (2.3) and (2.4).

Corollary 2.5 *The retaining probabilities in the pairwise and global approach are related as*

$$g_P(r) \leq g_G(r),$$

when the same radii and weight distributions are used in both cases.

3 Characteristics of the thinned processes

In this section we will look at some characteristics of the sphere process after thinning: the intensity of the points, the distribution of the sphere radii, and the so-called *volume fraction* of the union of all spheres. Let l_d denote the d-dimensional Lebesgue measure. The volume fraction of a stationary random closed set Ξ in d dimensions is defined by $p = \mathbf{E}(l_d(\Xi \cap [0,1]^d)) = \Pr(o \in \Xi)$, which for germ-grain models with non-overlapping spheres can be written as $p = \lambda\overline{V}$, where λ is the intensity of the grains and $\overline{V}$ denotes the mean volume for a typical grain.

In the sequel some formulae are equal in the pairwise and global case except for which of the probabilities $g_P(r)$ and $g_G(r)$ that is used. For simplicity we let $g(r)$ symbolize both $g_P(r)$ and $g_G(r)$ in such cases.

3.1 The intensity of the point process after thinning

By the definition of $g(r)$ it is clear that $\int_0^\infty g(r)F_{pr}(dr)$ is the retaining probability of a randomly chosen point of the original point process. Since the original point process is Poissonian we get the following theorem.

Theorem 3.1 *The intensity of the thinned point process is given by*

$$\lambda_{th} = \lambda \int_0^\infty g(r)F_{pr}(dr). \tag{3.1}$$

We see that $\lambda_{th} \leq \lambda$ and thus $\lambda_{th} \to 0$ when $\lambda \to 0$, whatever thinning procedure is used. However, if $\lambda \to \infty$, then the pairwise and global thinning procedures behave differently in some cases.

If the weights are random variables which are independent mutually and of the radii, then in the pairwise case we have by Theorem 2.1 and Theorem 3.1

$$\lambda_{th} \;=\; \lambda \int_0^\infty \exp\{-\lambda\kappa_d \Pr(W_1 \leq W_2) \int_0^\infty (r+y)^d F_{pr}(dy)\} F_{pr}(dr),$$

where W_1 and W_2 are independent weights, and $\lambda_{th} \to 0$ as $\lambda \to \infty$. In particular, if the weight distribution is continuous as in Corollary 2.2, then $\Pr(W_1 \leq W_2) = 1/2$ and

$$\lambda_{th} \;=\; \lambda \int_0^\infty \exp\{-\frac{\lambda\kappa_d}{2} \int_0^\infty (r+y)^d F_{pr}(dy)\} F_{pr}(dr) \to 0, \tag{3.2}$$

as $\lambda \to \infty$. For a given distribution F_{pr} we see that there exists a finite intensity for the original Poisson point process which gives a maximal rate for the thinned point process provided that the appropriate moments of F_{pr} exist. Note further that if these moments do not exist, for instance if in dimension 2 the second order moment of F_{pr} is infinite, then $g_P(r) = 0$ and the thinned process vanishes for all λ.

If the weights are continuous random variables which are independent of each other and of the radii, we have in the global case by Corollary 2.4 and (3.1)

$$\begin{aligned} \lambda_{th} \;&=\; \int_0^\infty \frac{1 - \exp\{-\lambda\kappa_d \int_0^\infty (r+y)^d F_{pr}(dy)\}}{\kappa_d \int_0^\infty (r+y)^d F_{pr}(dy)} F_{pr}(dr) \\ &\to\; \int_0^\infty \frac{1}{\kappa_d \int_0^\infty (r+y)^d F_{pr}(dy)} F_{pr}(dr), \end{aligned} \tag{3.3}$$

as $\lambda \to \infty$ if the dth moment of F_{pr} exists. Otherwise $g_G(r) = 0$ and the thinned process vanishes also in this case.

Hence, if the weights are continuous random variables which are independent mutually and of the radii, then $\lambda_{th} \to 0$ as $\lambda \to \infty$ in the pairwise case, while λ_{th} tends to a constant as $\lambda \to \infty$ in the global case. The special case of constant sphere radii r_0 is considered in the following examples.

Example 3.4. *Fixed radius, intersecting spheres removed.* In this case, which corresponds to fixed weights, $g_P(r_0) = g_G(r_0) = \exp\{-\lambda\kappa_d(2r_0)^d\}$ by Example 2.1. The intensity after thinning, $\lambda_{th} = \lambda g_P(r_0)$, is maximized if the original Poisson rate is $\lambda = (\kappa_d(2r_0)^d)^{-1}$, which gives $\lambda_{th} = (\kappa_d(2r_0)^d e)^{-1}$, and the volume fraction $\lambda_{th}\kappa_d r_0^d = (2^d e)^{-1}$. □

Example 3.5. *Fixed radius, pairwise thinning, uniformly distributed weights.* By (3.2) the intensity after thinning is $\lambda_{th} = \lambda \exp\{-\lambda\kappa_d(2r_0)^d/2\}$. It follows that $\lambda = 2(\kappa_d(2r_0)^d)^{-1}$ maximises λ_{th}. We then get $\lambda_{th} = 2(\kappa_d(2r_0)^d e)^{-1}$, and the volume fraction is $\lambda_{th}\kappa_d r_0^d = (2^{d-1}e)^{-1}$. □

Example 3.6. *Fixed radius, global thinning , uniformly distributed weights.* In this case λ_{th} increases with λ, and, by (3.3), $\lim_{\lambda\to\infty} \lambda_{th} = (\kappa_d(2r_0)^d)^{-1}$, and the volume fraction tends to 2^{-d} as $\lambda \to \infty$. □

3.2 The sphere radius distribution after thinning

Arguing in a similar fashion as for Theorem 3.1 gives the following theorem.

Theorem 3.2 *Let F_{pr} and F_{th} denote the distribution function of the radii before and after thinning. Then*

$$F_{th}(r) = 1 - k\int_r^\infty g(s)F_{pr}(ds),$$

with the constant k given by

$$k^{-1} = \int_0^\infty g(r)F_{pr}(dr).$$

Suppose in particular that the original sphere radius distribution is continuous with density f_{pr}. Then the distribution of the radii after thinning is also continuous with density given by

$$f_{th}(r) = kg(r)f_{pr}(r). \tag{3.4}$$

Let $h(r) = F'(r)/(1 - F(r))$ denote the hazard rate of a distribution with distribution function $F(r)$. In the following corollary we see that the right tail of the radius distribution is preserved if large spheres are kept. More precisely, the hazard rates of the thinned and the proposal radius distributions are asymptotically identical.

Corollary 3.3 *Suppose that a point and its associated d-dimensional sphere are kept if and only if the sphere meets no larger or equal sized sphere of the original marked point process. Suppose also that the original sphere radius distribution is continuous with hazard rate h_{pr} with $h_{pr}(r) > 0$ for $r > r_0$ for some r_0, and that the radius in the proposal distribution has finite moment of dth order. Then*

$$\lim_{r\to\infty} g(r) = 1, \tag{3.5}$$

and the hazard rate h_{th} of the thinned radius distribution is asymptotically identical to h_{pr} in the sense that

$$\lim_{r\to\infty} \frac{h_{th}(r)}{h_{pr}(r)} = 1. \tag{3.6}$$

Proof. Note that here pairwise and global assignment of weights coincide, and (3.5) follows from Example 2.2. Further, from (3.4) we get

$$h_{th}(r) = \frac{g(r)f_{pr}(r)}{\int_r^\infty g(s)f_{pr}(s)ds},$$

and now (3.6) also follows. ■

3.2.1 Exponential distribution in one dimension

In one dimension it turns out that in some cases we get particularly simple results if we start with an exponential distribution for the radii: when all

discs that intersect another disc are removed, or when we have a pairwise thinning with a continuous weight function which is independent of the radius. Assume thus that the proposal radius distribution is exponential with expectation μ_{pr}, that is $F_{pr}(r) = 1 - \exp(-r/\mu_{pr})$. In the case where we have a pairwise thinning with a continuous weight function which is independent of the radii,

$$g_P(r) \;\; = \;\; \exp\{-\lambda \int_0^\infty (r+y) F_{pr}(dy)\},$$

by Corollary 2.2. A simple calculation using Theorem 3.2 shows then that after thinning the radius distribution is exponential with expectation $\mu_{th} = \mu_{pr}/(1+\lambda\mu_{pr})$. Furthermore,

$$\lambda_{th} = \frac{\lambda \exp(-\lambda\mu_{pr})}{1+\lambda\mu_{pr}},$$

by (3.2), and the volume fraction is $2\lambda_{th}\mu_{th} = 2\lambda \exp(-\lambda\mu_{pr})\mu_{pr}/(1+\lambda\mu_{pr})^2$.

In the case where all discs that intersect another disc are removed, we similarly get, under the above assumptions, an exponential radius distribution after thinning with expectation $\mu_{th} = \mu_{pr}/(1+2\lambda\mu_{pr})$, and the point process intensity $\lambda_{th} = \lambda \exp(-2\lambda\mu_{pr})(1+2\lambda\mu_{pr})^{-1}$.

3.2.2 Truncated normal distribution in two dimensions

In two dimensions we similarly get simple results if the radius distribution is normal truncated at zero. Assume thus that the radius density is

$$f_{pr}(r) = (\sigma\Phi(\mu/\sigma))^{-1}\varphi(\frac{r-\mu}{\sigma}), \quad r > 0,$$

where Φ and φ are the distribution function and density of the standardized normal distribution, respectively . The expectation of this distribution is

$$\mu_{pr} = \mu + \sigma\varphi(\mu/\sigma)/\Phi(\mu/\sigma).$$

A straightforward calculation using Theorem 3.2 shows then that after pairwise thinning with a continuous weight function which is independent of the radius, the radius distribution is of the same type,

$$f_{th}(r) = (\sigma_{th}\Phi(\mu_{th}/\sigma_{th}))^{-1}\varphi(\frac{r-\mu_{th}}{\sigma_{th}}), \quad r > 0, \tag{3.7}$$

with $\sigma_{th}^2 = \sigma^2/(1+\pi\lambda\sigma^2)$ and

$$\mu_{th} = \frac{\mu}{1+\pi\lambda\sigma^2} - \pi\lambda\sigma_{th}^2\mu_{pr}.$$

If rather all discs that intersect each other are removed, then the radius distribution is as in (3.7) but with $\sigma_{th}^2 = \sigma^2/(1+2\pi\lambda\sigma^2)$ and $\mu_{th} = \mu(1+2\pi\lambda\sigma^2)^{-1} - 2\pi\lambda\sigma_{th}^2\mu_{pr}$.

3.2.3 Mixture model with two sphere sizes

Now we consider a mixture model of spheres with two different radii, r_1 and r_2, in $\mathbb{R}^d$. As in Sections 3.2.1 and 3.2.2 we let the weight distribution be continuous and independent of the radii. Here, however, we consider global thinning as $\lambda \to \infty$, so that the maximal volume fraction is obtained. Let p_i denote the probability of radius r_i in the proposal distribution, and $p_{th}(r_i)$ the probability of radius r_i after thinning. If $r_2 = yr_1$, $y > 0$, we get by Corollary 2.4 and Theorem 3.2

$$p_{th}(r_1) = \frac{p_1(2^d p_1 + (1+y)^d p_2)^{-1}}{p_1(2^d p_1 + (1+y)^d p_2)^{-1} + p_2((1+y)^d p_1 + (2y)^d p_2)^{-1}}.$$

As an example, Figure 2 shows the probability after thinning, $p_{th}(r_1)$, as a function of p_1 in the two-dimensional case when $r_2 = 2r_1$.

As expected, we see that the probability of the smaller sphere is larger after thinning than in the proposal distribution. The same phenomena was found by simulation in Meakin and Jullien (1992a,b) and Stoyan and Schlater (2000) for the RSA model.

3.2.4 Inversion of the radius distributions

In the previous sections we have seen that in some special cases it is possible to calculate explicitly the radius distribution F_{pr} of the unthinned spheres process from a desired distribution F_{th} of the thinned process. However, in general it seems as one can only hope for an iterative method for computing F_{pr} from F_{th}. Such a method will now be briefly sketched for the global case when the weight distribution is continuous and does not depend on the radius.

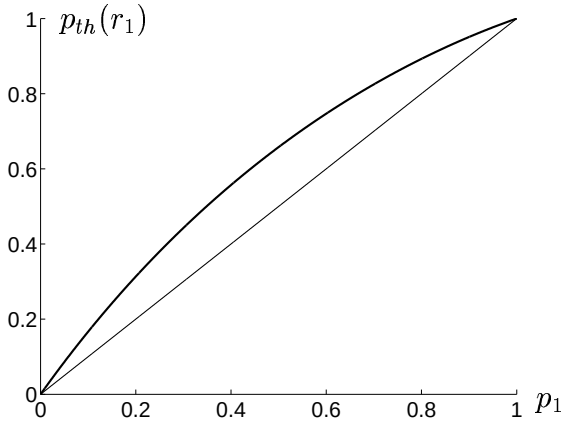

Figure 2: Probability of smaller sphere after thinning as function of the corresponding probability in the proposal distribution for a mixture model with two sphere sizes. The identity function is shown as reference.

Consider dimension $d = 2$ and assume that the proposal and thinned radius distributions have densities. For given thinned intensity λ_{th} and radius density f_{th} we wish to determine the corresponding proposal intensity $\lambda_{pr} = \lambda$ and radius density f_{pr}. Based on Corollary 2.4, Theorems 3.1 and 3.2 and (3.4) the following iteration step is suggested for obtaining an improved approximation $(\lambda_{pr,n+1}, f_{pr,n+1})$ of (λ_{pr}, f_{pr}) from a previous approximation $(\lambda_{pr,n}, f_{pr,n})$:

$$\begin{aligned}
B_n &= \int_0^\infty r f_{pr,n}(r) dr \\
C_n &= \int_0^\infty r^2 f_{pr,n}(r) dr \\
A_n(r) &= \lambda_{pr,n} \kappa_d (r^2 + 2rB_n + C_n) \\
g_n(r) &= (1 - e^{-A_n(r)})/A_n(r) \\
k_n &= \int_0^\infty \frac{f_{th}(r)}{g_n(r)} dr \\
\lambda_{pr,n+1} &= k_n \lambda_{th} \\
f_{pr,n+1}(r) &= \frac{f_{th}(r)}{k_n g_n(r)}.
\end{aligned}$$

In an example with an exponential thinned radius distribution this method

was empirically found to perform satisfactorily for $\lambda_{th} < \lambda_0$. With a unit expected thinned radius we found empirically $\lambda_0 \approx 0.030$. As an example with $\lambda_{th} = 0.028$ we found after 100 iterations $\lambda_{pr} = 0.0715$ and the proposal density function shown in the right part of Figure 3 together with the exponential thinned density. To start the iteration, we just put $(\lambda_{pr,0}, f_{pr,0}) = (\lambda_{th}, f_{th})$. From Figure 3 we see that the radius distribution is moved to the left in going from the proposal to the thinned density, cf. the comments in the end of Section 3.2.3.

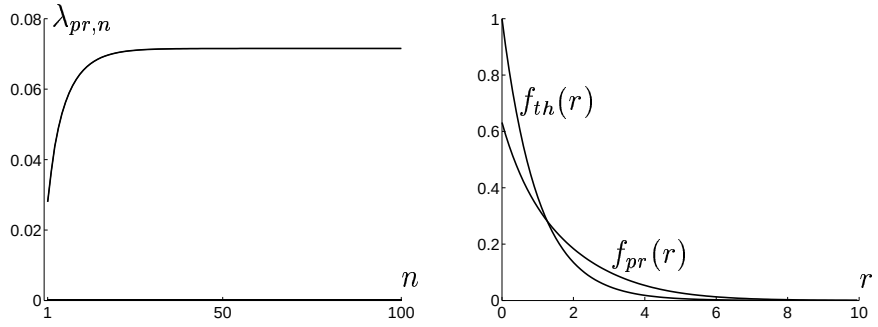

Figure 3: Left: proposal intensity approximations as a function of iteration number n. Right: proposal radius density computed by iteration for a unit-expectation exponential thinned density, which is also shown. The expectation of the computed proposal density is 1.566.

3.3 Simulations

We have simulated a two-dimensional Poisson process with intensity $\lambda = 1000$ in the unit square, and placed discs with exponentially distributed radii with expectation 0.01 at the points, and then carried out three different kinds of thinning. Figure 4 a) shows the process of discs before thinning, while all intersecting discs are removed in b), the larger disc is kept in the competition between two intersecting ones in c), and in d) we have carried out a global thinning with uniformly distributed weights. Some features of the different thinning procedures are illustrated in the figure. For instance, we showed in Section 3.1 that for the type of thinning used in Figure 4 b) , λ_{th} first increases and then tends to zero as $\lambda \to \infty$. This is the case also in Figure 4 c) where large discs are kept and the radius distribution is exponential, in

contrast to the case of global thinning and uniform weights in Figure 4 d), for which λ_{th} increases to a constant . When carrying out a series of simulations with increasing λ this behaviour is easily seen. Here we have just chosen one value of λ, which lies above the value which would give maximal λ_{th} in b), and just below it in c).

An obvious observation is that there are more large discs retained in c) than in b) and d). Moreover, the variation of disc sizes seems to be larger in this case.

When the intensity is low it is clear that whatever thinning procedure is used, the resulting point process is close to a Poisson process. As the intensity increases we believe that the resulting process tends to result in clusters of non-overlapping grains in some cases. In b), where all intersecting discs are removed, which corresponds to constant weights, such a clustering tendency can be seen.

One purpose of this simulation is to show that it might be reasonable to model the defects in cast iron (Figure 1) with some process proposed in this paper. A more careful study of data would suggest suitable λ_{th} and radius distribution after thinning, and based on this, the choice of proposal process and thinning mechanism could be made.

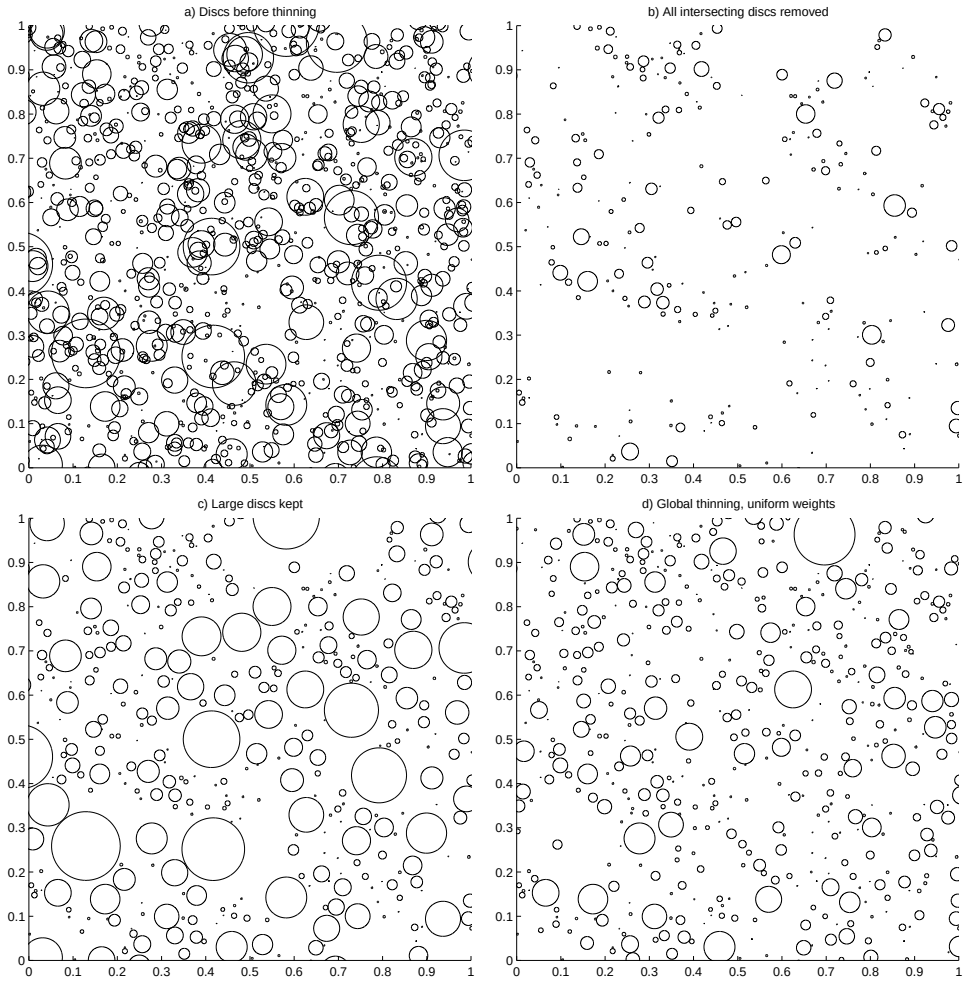

Figure 4: Simulation of a disc process before and after three different thinning procedures.

4 Non-spherical grains

4.1 Fixed orientations

In this section we derive expressions for the retaining probabilities $g_P(r)$ and $g_G(r)$ in the case where the grains have varying sizes but the same shape and

orientation as a convex set $C \subset \mathbb{R}^d$, which is not necessarily spherical. The only thing we need to do is to replace $\Pr(B_d(o,r) \cap B_d(X,y) \neq \emptyset)$ in (2.1) and (2.2) by the corresponding probability for the set C. To describe the size of a set, we use the diameter/2, where the *diameter* of a set $A \subset \mathbb{R}^d$ is defined to be the number

$$D(A) = \sup_{x,y \in A} |x - y|.$$

Let $\mathcal{C}^d$ denote the family of compact, convex sets C with interior points in $\mathbb{R}^d$, such that $o \in C$ and $D(C)/2 = 1$. Furthermore, let $C(z,r)$ denote a set with the same shape as C, translated by z and with diameter$/2 = r > 0$, that is $C(z,r) = \{ry + z : y \in C\}$, and $l_d(C(z,r)) = r^d l_d(C)$. To calculate $\Pr(C(o,r) \cap C(X,y) \neq \emptyset)$, recall from the proof of Theorem 2.1 that X is uniformly distributed in $B_d(o,x)$. It follows that

$$\begin{aligned} &\Pr(C(o,r) \cap C(X,y) \neq \emptyset) \\ &\quad = \Pr(X \in \{z : C(o,r) \cap C(z,y) \neq \emptyset\}) \\ &\quad = l_d(\{z : C(o,r) \cap C(z,y) \neq \emptyset\} \cap B_d(o,x))/l_d(B_d(o,x)). \end{aligned}$$

Without loss of generality we may assume that $\{z : C(o,r) \cap C(z,y) \neq \emptyset\} \subset B_d(o,x)$, since $g_P(r)$ and $g_G(r)$ are achieved as $x \to \infty$; thus

$$\Pr(C(o,r) \cap C(X,y) \neq \emptyset) \quad = \quad l_d(\{z : C(o,r) \cap C(z,y) \neq \emptyset\})/(x^d \kappa_d).$$

In some cases, as in the following examples, it is easy to find $l_d(\{z : C(o,r) \cap C(z,y) \neq \emptyset\})$.

Example 4.7. *Disc.* If $C \in \mathcal{C}^2$ is a disc, then $l_2(C) = \pi$, and the set $\{z : C(o,r) \cap C(z,y) \neq \emptyset\}$ is a disc of radius $r + y$. Hence

$$\Pr(C(o,r) \cap C(X,y) \neq \emptyset) = (r+y)^2 l_2(C)/(\pi x^2) = (r+y)^2/x^2.$$

In particular, with $y = r$ we get $\Pr(C(o,r) \cap C(X,r) \neq \emptyset) = 4r^2 l_2(C)/(\pi x^2)$. □

Example 4.8. *Triangle.* Let $C \in \mathcal{C}^2$ be an isosceles triangle, in which the sides perpendicular to each other have length $\sqrt{2}$ and $l_2(C) = 1$. Figure 5

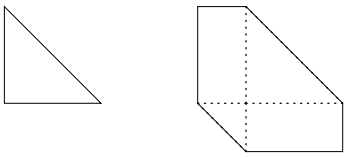

Figure 5: The sets $C(o,r)$ and $\{z : C(o,r) \cap C(z,y) \neq \emptyset\}$ when C is an isosceles triangle, and $y = r/2$.

shows the shape and size of $C(o,r)$ and of $\{z : C(o,r) \cap C(z,y) \neq \emptyset\}$. As seen by the figure this area is $r^2 + y^2 + 4ry$, and hence

$$\Pr(C(o,r) \cap C(X,y) \neq \emptyset) \quad = \quad (r^2 + y^2 + 4ry)/(\pi x^2).$$

In particular, if $r = y$ then $\Pr(C(o,r) \cap C(X,r) \neq \emptyset) = 6r^2 l_2(C)/(\pi x^2)$.

In fact, these formulae hold for any shape of the triangle C, see (4.6) below.

□

In order to derive $\Pr(C(o,r) \cap C(X,y) \neq \emptyset)$ for general convex C, we first need to introduce some set theory. For $A, B \subset \mathbb{R}^d$ and $c \in \mathbb{R}$ the *Minkowski sum* and *scalar multiple* are defined as

$$A + B = \{x + y : x \in A, y \in B\} \quad \text{and} \quad cA = \{cx : x \in A\},$$

respectively. If $c = -1$ we get $\check{A} = \{-x : x \in A\}$, which we call the *reflected set* of A. For $x \in \mathbb{R}^d$, $A + \{x\}$ is the *translate* of A by x. If $A = \check{A} + \{x\}$ for some $x \in \mathbb{R}^d$, A is said to be *centrally symmetric*. An alternative, and for us more useful, way of writing the Minkowski sum is

$$A + B = \{x \in \mathbb{R}^d : A \cap (\check{B} + \{x\}) \neq \emptyset\}. \tag{4.1}$$

For the set $xA + yB$, where $x, y \in \mathbb{R}^+$ and $A, B \subset \mathbb{R}^d$ are non-empty convex sets, the volume can be written as:

$$l_d(xA + yB) = \sum_{i=0}^{d} \binom{d}{i} x^i y^{d-i} \nu_{i,d-i}(A,B), \tag{4.2}$$

where $\nu_{i,d-i}(A,B) = \nu(\overbrace{A,\ldots,A}^{i},\overbrace{B,\ldots,B}^{d-i})$ are the *mixed volumes (areas in* $\mathbb{R}^2$*)* of A and B, (see e.g. Bonnesen and Fenchel (1948) p. 40). Note the special cases $\nu_{d,0}(A,B) = l_d(A)$ and $\nu_{0,d}(A,B) = l_d(B)$.

It can be shown that if A is a convex set, then

$$l_2(A) \leq \nu(A,\check{A}) \leq 2l_2(A), \quad A \subset \mathbb{R}^2, \tag{4.3}$$

and

$$l_3(A) \leq \nu(A,A,\check{A}) \leq 3l_3(A), \quad A \subset \mathbb{R}^3. \tag{4.4}$$

The lower bounds are attained if and only if A is centrally symmetric while the upper bounds are attained if and only if A is a triangle and a tetrahedron, respectively. For a proof of these facts, see e.g. Bonnesen and Fenchel (1948, p. 105), where inequalities corresponding to (4.3) and (4.4) in higher dimensions also can be found. To derive mixed volumes for arbitrary convex sets is not so easy. However, for centrally symmetric sets, such as discs and rectangles, and for triangles $\nu(A,\check{A})$ is given in (4.3), and for arbitrary polygons in $\mathbb{R}^2$ and $\mathbb{R}^3$ a simple formula can be found in Eggleston (1963, p. 85). For polytopes in $\mathbb{R}^d$, $d \geq 2$, a formula is given in Betke (1992).

Now we are ready to derive the thinning probabilities for convex $C \in \mathcal{C}^d$. Note that $\{z : C(o,r) \cap C(z,y) \neq \emptyset\}$ equals $C(o,r) + \check{C}(o,y)$ by (4.1), and thus

$$\begin{aligned} \Pr(C(o,r) \cap C(X,y) \neq \emptyset) &= l_d(C(o,r) + \check{C}(o,y))/l_d(B_d(o,x)) \\ &= \frac{1}{x^d \kappa_d} \sum_{i=0}^{d} \binom{d}{i} r^i y^{d-i} \nu_{i,d-i}(C,\check{C}), \end{aligned} \tag{4.5}$$

where the last equality follows from (4.2). What determines the probability is hence the volumes and the mixed volumes of the set and its reflection, where the mixed volumes are dependent on the shape of the set. In particular, in $\mathbb{R}^2$

$$\Pr(C(o,r) \cap C(X,y) \neq \emptyset) = \left((r^2+y^2)l_2(C) + 2ry\nu(C,\check{C})\right)/(\pi x^2).$$

By (4.3), we have for $C \in \mathcal{C}^2$,

$$\frac{(r+y)^2 l_2(C)}{\pi x^2} \leq \Pr(C(o,r) \cap C(X,y) \neq \emptyset) \leq \frac{((r+y)^2 + 2ry)l_2(C)}{\pi x^2}, \tag{4.6}$$

with equalities as in (4.3). Note that Examples 4.7 (circle) and 4.8 (triangle) are hence extremal, since the probabilities in these cases equal the left-hand and right-hand side in (4.6), respectively. In three dimensions, we get the following inequalities when $C \in \mathcal{C}^3$

$$\frac{(r+y)^3 l_3(C)}{\kappa_3 x^2} \leq \Pr(C(o,r) \cap C(X,y) \neq \emptyset) \leq \frac{((r+y)^3 + 6ry(r+y))l_3(C)}{\kappa_3 x^2},$$

with equalities as in (4.4) and $\kappa_3 = 4\pi/3$.

In the area of integral geometry, an expression for the volume $l_d(\{z : A \cap (B+z) \neq \emptyset\})$, where $A, B \subset \mathbb{R}^d$ are convex, was found already by Blaschke (1937) in $d = 2, 3$, and by Berwald and Varga (1937) in $d = 3$. In an arbitrary dimension the volume is given by Weil (1990) as a special case of a much more general formula. Hence the result (4.5) follows directly from these references.

To conclude this section, we formulate the above achievements as a theorem:

Theorem 4.1 *Theorems 2.1, 2.3, 3.1 and 3.2 and Corollaries 2.2, 2.4 and 3.3, with radius interpreted as diameter/2, hold true for convex grains with the same shape and orientation as $C \in \mathcal{C}^d$ if $(r+y)^d$ in $g_P(r)$ and $g_G(r)$ is replaced by $x^d Pr(C(o,r) \cap C(X,y) \neq \emptyset)$, given by (4.5).*

4.2 Random orientations

In the previous section all grains had the same shape and orientation; the case of random orientations may be more useful in some applications. To get a result corresponding to Theorem 4.1 in this case, we can use the so-called *principal kinematic formula* for convex sets, which gives a measure of the set of rotations and translations for one convex set such that it intersects another fixed convex set. For simplicity we just consider dimensions 2 and 3 here.

Let $S_{d-1}(C)$ denote the $(d-1)$-dimensional surface area and $\overline{b}(C)$ the so-called mean width of the convex set $C \subset \mathbb{R}^d$. The mean width can be defined as follows: For each line g through the origin, let $g(C)$ denote the smallest distance between two parallel hyperplanes perpendicular to g such that C is inbetween them. Then $\overline{b}(C)$ is the average value of $g(C)$ over all lines g. A

formula for the mean width of a general convex set can be found in Schneider (1993) p. 42, while a formula for the mean width of a convex polytope C in $\mathbb{R}^3$ is given in Santaló (1976) p. 226:

$$\overline{b}(C) = \frac{1}{4\pi} \sum_{i=1}^{m_C} (\pi - \alpha_i) l_i,$$

where m_C is the number of edges of C, l_i the lengths of the edges, and α_i the corresponding dihedral angles (i.e. the angles between adjacent sides).

A rotation about the origin is a map $m : \mathbb{R}^d \to \mathbb{R}^d$, which can be represented in the form $mx = \mathbf{A}x$, $x \in \mathbb{R}^d$, where $\mathbf{A}$ is an orthogonal matrix with det$\mathbf{A}$=1. By a uniformly distributed rotation we mean an element from the group of rotations about the origin, chosen according to a so-called Haar measure (see e.g. Miles (1965) for details). Let R_1 and R_2 be independently and uniformly distributed rotations about the origin. From the principal kinematic formula, which can be found in Schneider (1993), it follows that if $C \in \mathcal{C}^2$, then

$$\Pr(R_1(C)(o,r) \cap R_2(C)(X,y) \neq \emptyset) = \frac{l_2(C)(r^2+y^2) + ryS_1(C)^2/(2\pi)}{\pi x^2}, \quad (4.7)$$

and if $C \in \mathcal{C}^3$, then

$$\Pr(R_1(C)(o,r) \cap R_2(C)(X,y) \neq \emptyset) = \frac{l_3(C)(r^3+y^3) + ry(r+y)S_2(C)\overline{b}(C)/2}{4\pi x^3/3}. \quad (4.8)$$

Hence we get the following result:

Theorem 4.2 *Theorems 2.1, 2.3, 3.1 and 3.2 and Corollaries 2.2, 2.4 and 3.3, with radius interpreted as diameter/2, hold true for convex grains with the same shape as $C \in \mathcal{C}^d$ and random orientations if $(r+y)^d$ in $g_P(r)$ and $g_G(r)$ is replaced by $x^d Pr(R_1(C)(o,r) \cap R_2(C)(X,y) \neq \emptyset)$ given by (4.7) and (4.8) if $d = 2$ and $d = 3$, respectively.*

In Schneider (1993) the principal kinematic formula is given in an arbitrary dimension, and by means of this, Theorem 4.2 is easily generalized to higher dimensions.

We get lower bounds on the probabilities of nonempty intersections by means of the so-called isoperimetric inequality and Urysohn's theorem: for

any convex set $C \subset \mathbb{R}^d$,

$$\left(\frac{l_d(C)}{\kappa_d}\right)^{d-1} \leq \left(\frac{S_{d-1}(C)}{S_{d-1}(\{x \in \mathbb{R}^d : |x| = 1\})}\right)^d \tag{4.9}$$

and

$$\frac{l_d(C)}{\kappa_d} \leq \left(\frac{\overline{b}(C)}{2}\right)^d, \tag{4.10}$$

where there are equalities if and only if C is a sphere in $\mathbb{R}^d$. These inequalities, which can be found in e.g. Bonnesen and Fenchel (1948) p.75, yield

$$\Pr(R_1(C)(o,r) \cap R_2(C)(X,y) \neq \emptyset) \geq \begin{cases} 4\frac{l_2(C)}{\pi x^2}, & \text{if } d = 2, \\ 8\frac{l_3(C)}{4\pi x^3/3}, & \text{if } d = 3. \end{cases}$$

In contrary to the case with fixed orientations, the centrally symmetric sets do not all behave the same now – here the disc and sphere are the only shapes for which the lower bounds of the probability are attained. Furthermore, all triangles (tetrahedra) of the same area (volume) do not give the same probability now, and there is no shape which gives an upper bound. Think for instance of a triangle of a fixed area which is stretched out in one direction - the more it is stretched out the larger is the perimeter and the closer to 1 is the probability of a nonempty intersection.

Finally we give some examples of the involved geometrical quantities for some common shapes of C for which $D(C)/2 = 1$:

Dimension 2	Area $l_2(C)$	Perimeter $S_1(C)$	
Disc	π	2π	
Square	2	$4\sqrt{2}$	
Equilateral triangle	$\sqrt{3}$	6	
Dimension 3	**Volume $l_3(C)$**	**Surface area $S_2(C)$**	**Mean width $\overline{b}(C)$**
Sphere	$4\pi/3$	4π	2
Cube	$8/(3\sqrt{3})$	8	$\sqrt{3}$
Regular tetrahedron	$2\sqrt{2}/3$	$4\sqrt{3}$	$\frac{3}{\pi}(\pi - \arccos 3^{-1})$

4.3 Fixed orientations and fixed sizes

A set which is of interest in the case where all grains are of equal sizes is $C + \check{C} = \{x \in \mathbb{R}^d : C \cap (C + \{x\}) \neq \emptyset\}$, which is called the *difference set* of $C \subset \mathbb{R}^d$. If $C \in \mathcal{C}^d$, it is well-known that

$$2^d l_d(C) \leq l_d(C + \check{C}) \leq \binom{2d}{d} l_d(C), \tag{4.11}$$

where the lower bound is attained if and only if C is centrally symmetric, and the upper bound is attained if and only if C is a simplex (see p. 409 Schneider (1993)).

Recall that we have defined size of a set as its diameter/2. Assume that all grains are of size r_0. Then, by (4.5) and (4.2),

$$\begin{aligned} \Pr(C(o, r_0) \cap C(X, r_0) \neq \emptyset) &= r_0^d \sum_{i=0}^{d} \binom{d}{i} \nu_{i,d-i}(C, \check{C})/(x^d \kappa_d) \\ &= r_0^d l_d(C + \check{C})/(x^d \kappa_d), \end{aligned}$$

if $C \in \mathcal{C}^d$, and it follows that

$$\frac{r_0^d 2^d l_d(C)}{x^d \kappa_d} \leq \Pr(C(o, r_0) \cap C(X, r_0) \neq \emptyset) \leq \frac{r_0^d \binom{2d}{d} l_d(C)}{x^d \kappa_d},$$

with equalities as in (4.11).

In Section 3.1 we saw that in the case of spherical grains and global assignment of continuous weights which are independent of the radii, the intensity of the point process after thinning increases to a constant as the intensity before thinning tends to infinity. Furthermore, if the spheres are all of equal size, as in Example 3.6, the volume fraction tends to 2^{-d} as the intensity before thinning tends to infinity. Now we show that, as expected, also in the case of non-spherical grains of a fixed orientation, the intensity of the point process after thinning and the volume fraction tend to constants. However, these constants depend on the shape of the grains.

By Corollary 2.4, Theorems 3.1 and 4.1 we get a limit of the intensity after thinning corresponding to (3.3), if $C \in \mathcal{C}^d$. When the size of all grains is r_0,

this limit is $\left(r_0^d l_d(C+\check{C})\right)^{-1}$, and then the asymptotic value of the volume fraction, which we denote by $v_{G,max}(C)$, is

$$v_{G,max}(C) = \frac{l_d(r_0 C)}{r_0^d l_d(C+\check{C})} \quad = \quad \frac{l_d(C)}{l_d(C+\check{C})}.$$

By (4.11) this asymptotic volume fraction has the following bounds:

$$\frac{1}{\binom{2d}{d}} \leq \frac{l_d(C)}{l_d(C+\check{C})} \leq \frac{1}{2^d},$$

where the upper bound is attained if and only if C is centrally symmetric, and the lower bound is attained if and only if C is a simplex.

If we consider the case of pairwise assignment, and weights and sizes as above, then $\lambda_{th} = \lambda \exp\{-\lambda r_0^d l_d(C+\check{C})/2\}$. This intensity, and hence also the volume fraction, attains its maximal value if $\lambda = 2(r_0^d l_d(C+\check{C}))^{-1}$. That value of λ yields $\lambda_{th} = 2(r_0^d l_d(C+\check{C})e)^{-1}$, and the maximal volume fraction, which we denote by $v_{P,max}(C)$, is

$$v_{P,max}(C) = \frac{2 l_d(C)}{l_d(C+\check{C})e} = 2 v_{G,max}(C)/e.$$

In the spherical case, this result agrees with Example 3.5.

Theorem 4.3 *Assume that the weight distribution $F_{W|r}$ is continuous and does not depend on the size r. With the notation introduced above,*

$$v_{G,max}(C) = \frac{l_d(C)}{l_d(C+\check{C})} \quad \textit{and} \quad v_{P,max}(C) = 2 v_{G,max}(C)/e.$$

Furthermore,

$$\frac{1}{\binom{2d}{d}} \leq v_{G,max}(C) \leq \frac{1}{2^d},$$

where the upper bound is attained if and only if C is centrally symmetric, and the lower bound is attained if and only if C is a simplex.

4.4 Random orientations and fixed sizes

Now we consider random rather then fixed orientations of the grains. We assume that the grains are uniformly rotated independently of each other and of everything else.

In the global case, in two dimensions, we get by Corollary 2.4, Theorems 3.1 and 4.2

$$\lambda_{th} \;\to\; \left(2r_0^2 l_2(C) + r_0^2 S_1(C)^2/(2\pi)\right)^{-1},$$

as $\lambda \to \infty$ if the 2nd moment of F_{pr} exists and $C \in \mathcal{C}^2$. Then the volume fraction $v_{G,max}(C)$ tends to

$$v_{G,max}(C) \;=\; \frac{l_2(C)}{l_2(C)2 + S_1(C)^2/(2\pi)} \leq 1/4,$$

with equality if and only if C is a disc, by (4.9).

In three dimensions, we get

$$\lambda_{th} \;\to\; \left(2r_0^3 l_3(C) + r_0^3 S_2(C)\overline{b}(C)\right)^{-1},$$

as $\lambda \to \infty$ if the 3rd moment of F_{pr} exists and $C \in \mathcal{C}^3$, and the volume fraction tends to

$$v_{G,max}(C) = \frac{l_3(C)}{l_3(C)2 + S_2(C)\overline{b}(C)} \;\leq\; 1/8,$$

with equality if and only if C is a sphere, by (4.9) and (4.10).

In the pairwise case it follows, in a similar fashion as when the orientations are fixed, that

$$v_{P,max}(C) = 2v_{G,max}(C)/e,$$

in both two and three dimensions.

Theorem 4.4 *Assume that the weight distribution $F_{W|r}$ is continuous and does not depend on r. If the grains are independently and uniformly rotated, then*

$$v_{G,max}(C) \;=\; \begin{cases} \dfrac{l_2(C)}{l_2(C)2 + S_1(C)^2/(2\pi)} \leq 1/4, & \text{if } d = 2, \\ \dfrac{l_3(C)}{l_3(C)2 + S_2(C)\overline{b}(C)} \leq 1/8, & \text{if } d = 3, \end{cases}$$

with equalities if and only if C is a disc and a sphere, respectively, and

$$v_{P,max}(C) = 2v_{G,max}(C)/e.$$

5 Concluding remarks

In this paper we have discussed models for non-overlapping spheres. One advantage with some of our models is that they allow more explicit analytical results than many other models in the literature on non-overlapping spheres. Furthermore, our results for patterns of spheres generalize to patterns of convex grains. We have concentrated here on results on the intensity, the volume fraction and the size distribution after thinning. The results illustrate, for instance, that it is possible to obtain a rather large class of size distributions after thinning.

The simulations, see Figure 4, indicate that by proper choice of the thinning mechanism it should be possible to obtain a rather flexible class of patterns for the grain locations, e.g. exhibiting clustering. This could be investigated further by simulation. One could estimate, say, Ripley's K-function or the pair-correlation function to study deviations from a Poisson process. Furthermore, some measure for the dependence between grain sizes would be of interest to study, for instance the mark correlation function.

The inspiration to this paper came from problems to model inclusions in materials, such as cast iron. Some of the patterns simulated in Section 3.3 look similar to the real data in Figure 1. It would be interesting to choose the radius distribution, the intensity and the thinning method in more detail, to see if it is possible to obtain a good model for the data.

In connection with fatigue, large spheres are of particular interest since they are assumed to cause cracks. It seems therefore of interest to see if asymptotic properties can be derived for suitable extreme-value distributions of grain sizes, cf. Embrechts et al. (1997).

In Corollary 3.3 we saw that under some conditions the hazard rate before and after thinning are asymptotically equal, when large spheres are kept in the thinning step. It would be of interest to consider the convergence rate.

Acknowledgement

The present paper originates from discussions at the workshop on *Fatigue limit: Application of Stochastic Geometry and Extremes* organized in August 2000 by the Stochastic Centre, Gothenburg. It is a pleasure to thank the

workshop participants for stimulating ideas, in particular, Stefano Beretta who supplied the images shown in Figure 1.

References

Berwald, W. and Varga, O. (1937) Integralgeometrie 24, Über die Schiebungen im Raum. *Math. Z.* **42**, 710–736.

Betke, U. (1992) Mixed volumes of polytopes. *Arch. Math.* **58**, 388–391.

Beretta, S. (2000) Unpublished research. Politecnico di Milano.

Blaschke, W. (1937) Integralgeometrie 21, Über Schiebungen. *Math. Z.* **42**, 399–410.

Bonnesen, T. and Fenchel, W. (1948) *Theorie der Konvexen Körper.* Chelsea, New York.

Daley, D.J., Stoyan, H. and Stoyan, D. (1999) The volume fraction of a Poisson germ model with maximally non-overlapping spherical grains. *Adv. Appl. Prob.* **31**, 610–624.

Eggleston, H.G. (1963) *Convexity.* Cambridge University Press, London.

Embrechts, P., Klüppelberg, C. and Mikosch, T. (1997) *Modelling extremal events.* Springer, Berlin.

Häggström, O. and Meester, R. (1996) Nearest neighbour and hard sphere models in continuum percolation. *Random Structures Algorithms* **9**, 295–315.

Jeulin, D. (1998) Probabilistic models of structures. In *Probamat-21st Century: Probabilities and Materials. Tests, Models and Applications for the 21st Century* ed. G.N. Frantziskonis, Kluwer Academic Publishers, Dordrecht, 233–257.

Mase, S. (1985) On the possible form of size distributions for Gibbsian processes of mutually non-intersecting discs. *J. Appl. Prob.* **23**, 649–659.

Matérn, B. (1960) Spatial variation. *Meddelanden från Statens Skogsforskningsinstitut.* **49** (5), 1–144. (Reprinted in Matérn, 1986.)

Matérn, B. (1986) *Spatial variation.* Lecture Notes in Statistics 36. Springer-verlag, Berlin.

Meakin, P. and Jullien, R. (1992a) Random-sequential adsorption of disks of different sizes. *Phys. Rev. A* **46**, 2029–2038.

Meakin, P. and Jullien, R. (1992b) Random sequential adsorption of spheres of different sizes. *Phys. A* **187**, 475–488.

Miles, R.E. (1965) On random rotations in $\mathbb{R}^3$. *Biometrika* **52**, 636–639.

Murakami, Y. and Beretta, S. (1999) Small defects and inhomogeneities in fatigue strength: experiments, models and statistical implications. *Extremes* **2**, 123–147.

Reiss, H., Frisch, H.L. and Lebowitz, J. (1959) Statistical mechanics of rigid spheres. *J. Chem. Phys.* **31**, 369–380.

Resnick, S. (199): Extreme values, regular variation and point processes. Springer, 1987.

Santaló, L. A. (1976) *Integral Geometry and Geometric Probability.* Addison-Wesley, Reading, Massachusetts.

Schneider, R. (1993) *Convex bodies: the Brunn-Minkowski theory*, Cambridge University Press, New York.

Stienen, H. (1982) *Die Vergroeberung von Karbiden in reinen Eisen-Kohlenstoff Staehlen.* Dissertation, RWTH Aachen.

Stoyan, D. (1990) Stereological formulae for a random system of non-overlapping spheres. *Statistics* **22**, 449–462.

Stoyan, D. (1998) Random sets: models and statistics. *Internat. Statist. Rev.* **66**, 1–27.

Stoyan, D., Kendall,W.S. and Mecke, J. (1995) *Stochastic Geometry and its Applications.* Second Edition, Wiley, Chichester.

Stoyan, D. and Schlater, M. (2000) Random sequential adsorption: Relationship to dead leaves and characterization of variability. *J. Statist. Phys.* **100**, 969–979.

Stoyan, D. and Stoyan, H. (1985) On one of Matérn's hard-core point process models. *Math. Nachr.* **122**, 205–214.

Talbot, J., Tarjus, G., Van Tassel, P.R. and Viot,P. (2000) From car parking to protein adsorption: an overview of sequential adsorption processes. *Colloids and Surfaces A* **165**, 287–324.

Torquato, S.(1995) Nearest neighbor statistics for packings of hard spheres and disks. *Phys. Rev. E* **51**, 3170–3182.

Weil, W. (1990) Iterations of translative formulae and non-isotropic Poisson processes of particles. *Math. Z.* **205**, 531–549.

Zoughi, R., Huber, C., Qaddoumi, N., Ranu, E., Otashevich, V., Mirshahi, R., Ganchev, S. and Johnson, T. (1997) Real-time and on-line microwave inspection of surface defects in rolled steel, *Proc. of the Asia-Pacific Microwave Conf., APMC'97, Hong Kong*, 1081–1084.